

PAPER • OPEN ACCESS

Contact heat transfer of a cutting diamond wheel with a boundary layer of air

To cite this article: A Bespalova *et al* 2021 *IOP Conf. Ser.: Mater. Sci. Eng.* **1164** 012013

View the [article online](#) for updates and enhancements.

Contact heat transfer of a cutting diamond wheel with a boundary layer of air

A Bespalova^{1,*}, O Faizulyna¹, V Lebedev², O Frolenkova² and T Chumachenko²

¹Odessa State Academy of Civil Engineering and Architecture, 4, Didrichsona St., Odessa, 65029, Ukraine

²Odessa National Polytechnic University, 1, Shevchenko avenue, Odessa, 65044, Ukraine

*E-mail: bespalova.a.v.2015@gmail.com

Abstract. Cutting of natural and artificial building materials is most often carried out with diamond cutting wheels on a metal base at cutting speeds of about 50-80 m/s. The intensity of the cutting process causes a significant heat release, as a result of which the wheel temperature rises to unacceptable values. The value of these unacceptable temperatures is about 600 - 650°C.

At these temperatures, graphitization of diamond grains occurs, i.e. loss of diamond layer and loss of cutting properties. In addition, a thin diamond wheel (thickness 1 - 3 mm) is deformed, which leads to jamming and its tensile strength at these temperatures is reduced by half, which creates the risk of rupture by centrifugal forces. In this work, it is taken into account that during the rotation of the wheel, a boundary layer of air is created around it, which is stationary relative to the wheel. Consequently, contact heat transfer occurs between the wheel and the boundary layer, and then convective heat transfer occurs between the boundary layer and the surrounding air. This scheme allows you to more accurately determine the time of safe operation of the diamond wheel. Contact heat transfer between the wheel and the boundary layer is not effective enough to lower the temperature. When air with a negative temperature is introduced into the boundary layer by means of a Rank-Hillsch tube, the wheel temperature decreases by about 10%.

When a sprayed coolant (fog cooling) is introduced into the boundary layer by means of an ejector tube, the wheel temperature decreases by 25%, which ensures an increase in the time of continuous operation.

1. Introduction

Cutting of natural and artificial building materials is most often carried out with diamond cutting wheels on a metal base at cutting speeds of about 50-80 m/s. The intensity of the cutting process causes a significant heat release, as a result of which the wheel temperature rises to unacceptable values. The value of these unacceptable temperatures is about 600 - 650 °C.

At these temperatures, graphitization of diamond grains occurs, i.e. loss of diamond layer and loss of cutting properties. In addition, a thin diamond wheel (thickness 1 – 3 mm) is deformed, which leads to jamming and its tensile strength at these temperatures is reduced by half, which creates the risk of rupture by centrifugal forces.

Thus, the heating temperature of the wheel should not exceed 600 °C. Therefore, the operating time of a diamond cutting disc is the time during which it is heated during continuous operation to a temperature of 600 °C. The longer this time, the higher the resistance of the diamond blade. In the present work, mathematical modeling is performed taking into account contact heat transfer between a rotating wheel and a boundary layer

The simulation of the process of interaction of the wheel with the environment is carried out according to the results of which it is possible to determine the time of wheel performance. However, in this paper, convective heat transfer between the wheel and the surrounding air is considered at a



time when the heat transfer process is more complex. When the wheel rotates around it, a boundary layer of air is created that is stationary relative to the wheel. Consequently, contact heat transfer occurs between the wheel and the boundary layer, and then convective heat transfer occurs between the boundary layer and the surrounding air. This scheme allows you to more accurately determine the time of safe operation of the diamond wheel.

2. References review

A significant number of research works devoted to this subject firstly consider convective heat transfer between the wheel and air, moreover, at high Reynolds numbers, which does not correspond to our case. Works [1-12] precisely consider precisely such cases, therefore, the data presented in these works cannot be used in our studies.

2.1. Research Methodology

The purpose of this work is to investigate the contact heat transfer process between a wheel and a boundary layer of air, based on which to determine the possibilities of cooling a rotating wheel by changing the thermophysical characteristics of the boundary layer.

The tasks to be solved in this article are as follows.

1. Mathematical modeling of the heat transfer process to determine the intensity of the latter.
2. Mathematical modeling of the wheel cooling process when changing the thermophysical characteristics of the boundary layer.

Calculations are carried out in accordance with the scheme presented in Figure1.

Here is a solution for a thin rotating wheel heated at the end in the contact area and cooled from the side surfaces as a result of contact heat exchange with the boundary layer. Figure 1 [13, 14].

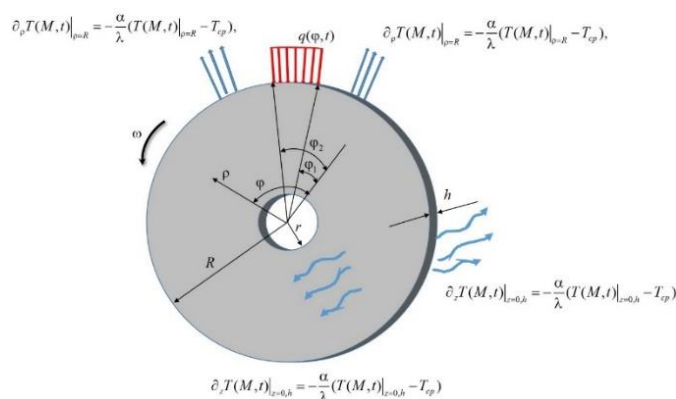


Figure 1. Design scheme for cooling of a rotating wheel.

A thick wheel with thickness h rotates in a plane XOY with angular velocity ω . At the end of the circle, within the limits of the contact arc, a heat source of intensity $q(\varphi, t)$ is defined, depending on the cutting conditions. On the lateral surfaces of the wheel and outside the contact arc, heat transfer occurs at the end according to the Newton-Richmann law, and on the lateral surfaces of the wheel heat transfer is considered not with the environment, but with the boundary layer, the temperature of which can be varied over a wide range up to -50°C .

The boundary-value heat conduction problem for a thin wheel in the presence of heat transfer through the side surfaces, taking into account the angular velocity in the polar coordinate system (ρ, φ) , has the form:

$$\begin{aligned} \partial_t T &= \alpha(\partial_\rho^2 + \rho^{-1}\partial_\rho + \rho^{-2}\partial_\varphi^2)T + \nu_\rho \partial_\rho T + \omega \partial_\varphi T - \frac{2\alpha_*}{\rho cb}(T - T_{bl}), \\ \partial_\rho &= \frac{\partial}{\partial \rho}, \quad \partial_\varphi = \frac{\partial}{\partial \varphi}, \quad \partial_t = \frac{\partial}{\partial t}, \quad T \equiv T(\rho, \varphi, t). \end{aligned} \tag{1}$$

Initial condition

$$T(\rho, \varphi, t)|_{t=0} = T_0. \tag{2}$$

Boundary conditions

$$\begin{aligned} \lambda \partial_\rho T(M, t)|_{\rho=R} + \alpha(T(M, t)|_{\rho=R} - T_{cp}) &= 0, \quad \varphi \in [\varphi_1, \varphi_2], \\ \partial_\rho T(M, t)|_{\rho=R} &= -\frac{q(\varphi, t)}{\lambda}, \quad \varphi \in [\varphi_1, \varphi_2], \end{aligned} \tag{3}$$

where T_{bl} boundary layer temperature; T_0 initial wheel temperature; α_* —coefficient of convective heat transfer between rotating disc and boundary layer; c – specific heat, (J/kg·grad); ρ - substance density (kg/m³) ρc – (J/m³·deg); α – coefficient of heat output; λ – coefficient of thermal conductivity; b – wheel thickness; T_{cp} – ambient temperature.

Using substitution

$$T(M, t) = \Theta(M, t) \exp\left(-\frac{\omega \rho}{2a} \varphi - \frac{\omega^2}{4a} t\right).$$

The boundary problem equations (1) - (3) is modified to the form:

$$\partial_t \Theta(M, t) = \alpha(\partial_r^2 + r^{-1}\partial_r + r^{-2}\partial_\varphi^2)\Theta(M, t) - \frac{2\alpha}{\rho ch}(\Theta(M, t) - T_{cp}), \quad M = M(r, \varphi). \tag{4}$$

$$\Theta(M, t)|_{t=0} = \Theta_0,$$

$$\lambda \partial_\rho \Theta(M, t)|_{\rho=R} = -\alpha(\Theta(M, t)|_{\rho=R} - T_{cp}), \quad \varphi \in [\varphi_1, \varphi_2], \tag{5}$$

$$\partial_\rho \Theta(M, t)|_{\rho=R} = f(\varphi, t), \quad f(\varphi, t) = \frac{q(\varphi, t)}{\lambda} \partial_r \exp\left(\frac{1}{2\alpha} rv + \frac{1}{4\alpha}\right) \sum_{j=1}^2 \nu_j^2, \quad \varphi \in [\varphi_1, \varphi_2].$$

In order to avoid the application of the Laplace transform and the difficulties with its treatment, we proceed as follows. We divide the time interval T into M intervals of length $h = TM^{-1}$ and replace the time derivative by the difference relation

$$\partial_t \Theta(r, \varphi, t) = \frac{\Theta_j(r, \varphi) - \Theta_{j-1}(r, \varphi)}{h}, \quad \Theta_j(r, \varphi, jh), \quad j = 1, 2, \dots$$

then

$$(\partial_\rho^2 + r^{-1}\partial_\rho + r^{-2}\partial_\varphi^2)\Theta_j(r, \varphi) - \mu^2 \Theta_j(r, \varphi) = F_j(r, \varphi), \tag{6}$$

$$\Theta(M, t)|_{t=0} = \Theta_0,$$

$$\lambda \partial_\rho \Theta(M, t)|_{\rho=R} = -\alpha(\Theta(M, t)|_{\rho=R} - T_{cp}), \quad \varphi \in [\varphi_1, \varphi_2], \tag{7}$$

$$\lambda \Theta(M, t)|_{\rho=R} = f(\varphi, t), \quad f(\varphi, t) = \frac{q(\varphi, t)}{\lambda} \partial_\rho \exp\left(\frac{1}{2\alpha} rv + \frac{t}{4\alpha} \sum_{j=1}^2 \nu_j^2\right), \quad \varphi \in [\varphi_1, \varphi_2],$$

where

$$\mu^2 = \frac{2\alpha}{\rho\alpha ch} + \frac{1}{h\alpha}, \quad F_j(r, \varphi) = T_{cp} - (h\alpha)^{-1} \Theta_{j-1}(r, \varphi).$$

Let us construct a discontinuous solution [15] of the heat equation for an unbounded plane $0 \leq \rho < \infty, |\varphi| < \pi$ containing a circular defect occupying the region $r = R, -\pi \leq \varphi \leq \pi$, upon transition through which they suffer discontinuities of continuity of the first kind, the temperature $\Theta_j(\rho, \varphi)$ and the heat flux $\partial_\rho \Theta_j(\rho, \varphi)$ with given jumps.)

$$\begin{aligned} \Theta_j(R+0, \varphi) - \Theta_j(R-0, \varphi) &= \langle \Theta(R, \varphi) \rangle, \\ \partial_\rho \Theta_j(R+0, \varphi) - \partial_\rho \Theta_j(R-0, \varphi) &= \langle \partial_\rho \Theta_j(R, \varphi) \rangle, \end{aligned} \tag{8}$$

those, a solution that satisfies the heat equation everywhere except for defect points. At these points, jumps in temperature and heat flux are set.

To construct a discontinuous solution of equation (6) with jumps equation (8), we apply the finite Fourier transform in the variable φ :

$$\Theta_j(\rho, \varphi) = \sum_{n=-\infty}^{\infty} \Theta_{j,n}(\rho) e^{in\varphi}, \quad \Theta_{j,n}(\rho) = \Phi_n[\Theta_j] \equiv \frac{1}{2\pi} \int_{-\pi}^{\pi} \Theta_j(\rho, \varphi) e^{in\varphi} d\varphi, \quad j=1, 2, \dots$$

and, Hankel transform, according to a generalized scheme [15]:

$$\Theta_{n,a}^j = \int_0^\infty \rho \Theta_{j,n}(\rho) J_n(a\rho) d\rho = \left(\int_0^{R=0} + \int_{R+0}^\infty \right) \rho \Theta_{j,n}(\rho) J_n(a\rho) d\rho,$$

where $J_n(z)$ – Bessel function.

As a result, we obtain:

$$\Theta_{n,a}^j = \frac{R}{a^2 + \mu^2} \left\{ J_n(\alpha R) \langle \partial \Theta_{j,n}(R) \rangle - \langle \Theta_{j,n}(R) \rangle \partial_r J_n(\alpha R) \right\} + \frac{F_{n,\alpha}^j}{a^2 + \mu^2}.$$

where $F_{n,\alpha}^j = \int_0^\infty \rho F_{j,n}(\rho) J_n(\alpha\rho) d\rho, \quad F_{j,n}(\rho) = \Phi_n[F_j(\rho, \varphi)].$

After reversing the Hankel transform, the required discontinuous solution of the heat equation in Fourier transforms can be written as:

$$\begin{aligned} \Theta_{j,n}(\rho) &= R \left\{ \langle \partial \Theta_{j,n}(R) \rangle G_{n,\lambda}(\rho, R) - \langle \Theta_{j,n}(R) \rangle \partial_\rho G_{n,\lambda}(\rho, R) \right\} + F_{j,n}(\rho), \\ G_{n,\lambda}(\rho, R) &= \int_0^\infty \frac{\alpha J_n(\alpha\rho) J_n(\alpha R)}{\alpha^2 + \tilde{\mu}^2} d\alpha, \quad F_{j,n}(\rho) = \int_0^\infty \frac{\alpha J_n(\alpha\rho) F_{n,\alpha}^j}{\alpha^2 + \tilde{\mu}^2} d\alpha. \end{aligned} \tag{9}$$

Taking into account that:

$$\left\{ \langle \Theta_{j,n}(R) \rangle, \langle \partial \Theta_{j,n}(R) \rangle \right\} \equiv \frac{1}{2\pi} \int_{-\pi}^{\pi} \left\{ \langle \Theta_j(R, \psi) \rangle, \langle \partial \Theta_j(R, \psi) \rangle \right\} e^{im\psi} d\psi.$$

We write the discontinuous solution equation (9) in the form:

$$\begin{aligned} \Theta_j(\rho, \varphi) &= \frac{R}{2\pi} \left\{ \int_{-\pi}^{\pi} \chi_j^{1-}(\psi) G_{n,\lambda}(\rho, R) e^{im\psi} d\psi - \int_{-\pi}^{\pi} \chi_j^{2-}(\psi) \partial_R G_{n,\lambda}(\rho, R) e^{im\psi} d\psi \right\} + F_{j,n}(\rho), \\ \chi_j^{1-}(\psi) &= \langle \Theta_j(R, \psi) \rangle, \quad \chi_j^{2-}(\psi) = \langle \partial \Theta_j(R, \psi) \rangle. \end{aligned}$$

Using the inverse finite Fourier transform formula, by φ , and the addition theorem [16].

$$\sum_{n=-\infty}^{\infty} J_n(\alpha r) J_n(\alpha R) e^{in\varphi} = J_0(\alpha, r_*), \quad r_*^2 = r^2 + R^2 - 2rR \cos \varphi.$$

we obtain:

$$\Theta_j(r, \varphi) = \frac{R}{2\pi} \left\{ \int_{-\pi}^{\pi} \chi_j^{1-}(\psi) K(\rho, R, \varphi - \psi) d\psi - \partial_\rho \int_{-\pi}^{\pi} \chi_j^{1-}(\psi) K(\rho, R, \varphi - \psi) d\psi \right\} + F_j(\rho, \varphi).$$

If we use equation (17) from [2], we obtain

$$K(\rho, R, \varphi) = \int_0^\infty \frac{\alpha J_0(\alpha, r_*)}{\alpha^2 + \mu} d\alpha = K_0(r_*, \mu).$$

Then:

$$\Theta_j(r, \varphi) = \frac{R}{2\pi} \left\{ \partial_R \int_{-\pi}^{\pi} \chi_1^{1-}(\psi) K_0(r_*, \tilde{\mu}) d\psi - \int_{-\pi}^{\pi} \chi_2^{1-}(\psi) K_0(r_*, \tilde{\mu}) d\psi \right\} + F_j(\rho, \varphi). \tag{10}$$

We illustrate the technique of using discontinuous solutions to solve the boundary value problem. This technique is based on the idea that the boundary of the wheel $\rho = R$ be considered a defect. We consider the third boundary value problem:

$$\Theta_j(R-0, \varphi) + \kappa \partial_\rho \Theta_j(R-0, \varphi) = f_j(\varphi). \tag{11}$$

Given that outside the domain specified in the conditions of the problem, the solution is identical to zero, i.e. a $\rho \succ R$, $\Theta_j(\rho, \varphi) \equiv 0$, и $(\Theta_j(R+0, \varphi) = \partial_\rho \Theta_j(R+0, \varphi) = 0)$, then on the basis of equation (11), we can write the following:

$$\chi_j^{2,-} = \langle \partial_\rho \Theta_j(R, \varphi) \rangle = -\kappa^{-1} (f_j(\varphi) - \Theta_j(R-0, \varphi)), \kappa = \lambda / \alpha. \tag{12}$$

As a solution to the boundary value problem equations (6), (12), we will use the discontinuous solution equation (10) with the jumps obtained here:

$$\Theta_j(r, \varphi) = \frac{R}{2\pi} \left\{ -\partial_R \int_{-\pi}^{\pi} \chi_j^{1-}(\psi) K_0(r_*, \tilde{\mu}) d\psi + \int_{-\pi}^{\pi} \frac{f_j(\varphi) - \Theta_j(R-0, \varphi)}{\kappa} K_0(r_*, \tilde{\mu}) d\psi \right\} + F_j(\rho, \varphi). \tag{13}$$

To get an equation to determine an unknown boundary value: $\chi_j^{1-}(\psi) = \Theta_j(R-0, \varphi)$, make the limit transition in equation (13) $\rho \rightarrow R-0$, considering that:

$$\lim_{\rho \rightarrow R} K_0(\mu \sqrt{\rho^2 + R^2 - 2\rho \cos(\varphi - \psi)}) = K_0(\mu 2^{1/2} R \sqrt{1 - \cos(\varphi - \psi)}) = K_0(\mu 2R |\sin(\varphi - \psi) / 2|).$$

And that $\sin(\varphi - \psi) / 2 \approx (\varphi - \psi) / 2$, at $\varphi \rightarrow \psi$, as well as representing the MacDonald function as:

$$K_0(z) = \ln\left(\frac{2}{z}\right) + \ln\left(\frac{2}{z}\right) + \sum_{m=0}^{\infty} \left(\frac{z}{2}\right)^m \frac{1}{\Gamma(m+1)m!} + \sum_{m=0}^{\infty} \left(\frac{z}{2}\right)^m \frac{\psi(m+1)}{(m!)^2}.$$

We can say that:

$$\left[\partial_\rho \int_{-\pi}^\pi \chi_j^{1-}(\psi) K_0(r_* \mu) d\psi \right]_{\rho=R \pm 0} = \frac{\nu \chi_j^{1-}(\phi)}{2} : \nu = -1 - \frac{\gamma}{2},$$

where γ – Euler constant.

As a result, we obtain:

$$\Theta_j(\rho, \phi) = \frac{R}{2\pi} \left\{ \int_{-\pi}^\pi \frac{f_j(\psi) - \chi_j^{1-}(\psi)}{\kappa} K_0(\mu |\sin(\phi - \psi) / 2|) d\psi \right\} + \frac{\nu \chi_j^{1-}(\phi)}{2} + F_j(R, \phi).$$

This relation can be written as an integral equation:

$$\chi_j^{1-}(\phi) + \frac{R}{2\pi} \int_{-\pi}^\pi \frac{f_j(\psi) - \chi_j^{1-}(\psi)}{\kappa(\nu - 2)} K_0(\mu |\sin(\phi - \psi) / 2|) d\psi + \frac{\nu \chi_j^{1-}(\phi)}{2} = F_j(R, \phi).$$

Using the MacDonald function representation, in the form:

$$K_0(\mu |\sin(\phi - \psi) / 2|) = \int_0^\infty \frac{\alpha}{\alpha^2 + \mu^2} \sum_{n=-\infty}^\infty J_n(\alpha R) J_n(\alpha R) e^{in(\phi - \psi)} da$$

we apply the finite Fourier transform to this equation, taking into account its properties and the convolution theorem:

$$\Phi_n[\partial_\phi^k f] = (in)^k \Phi_n[f], \Phi_n[f] = \int_{-\pi}^\pi f(\zeta) h(\phi - \zeta) d\zeta = 2\pi f_n h_n, \Phi_n[e^{im\phi}] = \frac{1}{2\pi} \int_{-\pi}^\pi e^{i\phi(m-n)} d\phi = \delta_{m,n}$$

We obtain:

$$\begin{aligned} \chi_{j,n}^{1-} &= \tau_n^{-1} [F_{j,n} - f_{j,n}], \tau_n = 1 - \frac{R}{\kappa(\nu - 2)} h_n, \\ h_n &= \int_0^\infty \frac{a}{a^2 + \mu^2} \sum_{m=-\infty}^\infty J_m(aR) J_m(aR) \int_{-\pi}^\pi e^{i(m-n)\phi} d\phi = \int_0^\infty \frac{\alpha [J_m(\alpha R)]^2}{a^2 + \mu^2}, \\ f_{j,n} &= \int_{-\pi}^\pi f_j(\Psi) e^{in\phi} d\phi, F_{j,n} = \int_{-\pi}^\pi F_{j,n}(R, \phi) e^{in\phi} d\phi. \end{aligned}$$

Inverting the Fourier transform [16], we obtain:

$$\chi_{j,n}^{1-} = \int_{-\pi}^\pi (F_j(\eta) - f_j(\eta)) \sum_{n=-\infty}^\infty \frac{e^{-in(\phi - \eta)}}{\tau_n} d\eta. \tag{14}$$

We introduce the unknown function $\psi(\phi)$, then the boundary conditions equation (7) are written as follows:

$$\begin{aligned} \Theta_j(R + 0, \phi) + \kappa \partial_\rho \Theta_j(R + 0, \phi) &= g_-(\phi) + \psi_+(\phi), \\ g_-(\phi) &= 0, |\phi| \in (\phi_1, \phi_2), g_+(\phi) = g(\phi), |\phi| \in (\phi_1, \phi_2), \\ \psi_+(\phi) &= \psi(\phi), |\phi| \in (\phi_1, \phi_2), \psi_-(\phi) = 0, |\phi| \in (\phi_1, \phi_2). \end{aligned} \tag{15}$$

If we assume that the functions $g_-(\varphi)$ and $\psi_+(\varphi)$ are known, then we pass to the third main boundary-value problem, the solution of which was obtained above. Using equation (14), we can write the following:

$$\Theta_j(R-0, \varphi) = - \int_{-\pi}^{\pi} (g_-(\eta) + \psi_+(\eta)) \Psi(\varphi - \eta) d\eta + \int_{-\pi}^{\pi} F_j(\eta) \Psi(\varphi - \eta) d\eta,$$

$$\Psi(\varphi - \eta) = \sum_{n=-\infty}^{\infty} \frac{e^{-in(\varphi-\eta)}}{\tau_n} d\eta.$$

Now satisfying the first boundary condition from equation (7) and taking into account equation (15) we obtain the integral equation:

$$\frac{\partial}{\partial \varphi} \int_{\varphi_1}^{\varphi_2} \Psi_j(\eta) \Psi(\varphi - \eta) d\eta = F(\varphi),$$

$$F(\varphi) = \int_{-\pi}^{\pi} F_j(\eta) \Psi(\varphi - \eta) d\eta - \frac{\partial}{\partial \varphi} \left(\int_{-\pi}^{\varphi_1} + \int_{\varphi_2}^{\pi} \right) g(\eta) \Psi(\varphi - \eta) d\eta.$$

In Figures 2–4 show plots of temperature changes depending on the polar angle φ and radius ρ and various values of the temperature of the boundary layer T_{bl} ; moreover, Figure 2 show plots at an angular velocity of $\omega r = 50m/s$, and in Figure 3 at $\omega r = 80m/s$. The temperature of the boundary layer was varied using the Ranque-Hills tube. The temperature was determined at an operating time of 60 s.

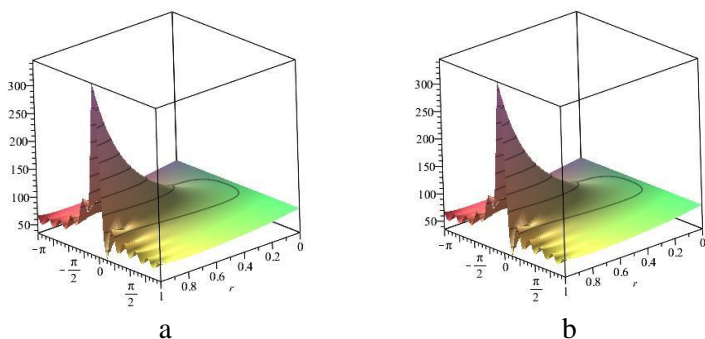


Figure 2. a) The temperature of the wheel at the temperature of the boundary layer + 200 °C; b) the temperature of the wheel at the temperature of the boundary layer -500 °C. $V_{wheel} = 50 m/s$.

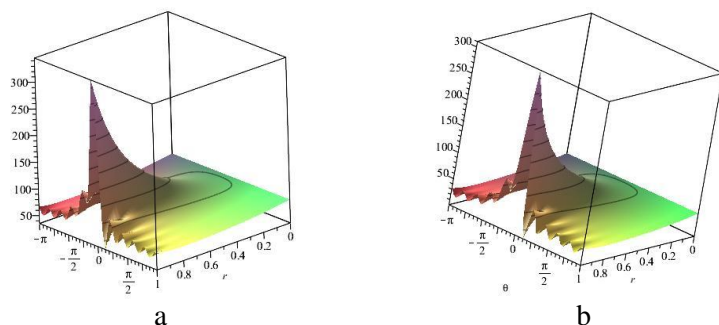


Figure 3. a) The temperature of the wheel at the temperature of the boundary layer + 20° C; b) the temperature of the wheel at the temperature of the boundary layer -50° C. $V_{wheel} = 80 m/s$.

Additional mathematical modeling of the process of introducing the boundary layer of atomized coolant (fog) showed that the temperature of the wheel decreases significantly, as shown in Figure 4.

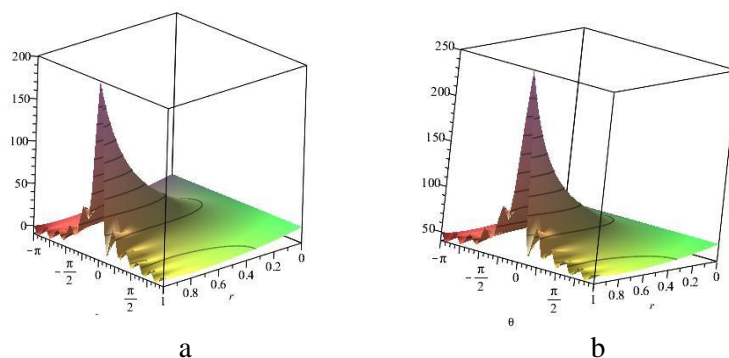


Figure 4. a) Circle temperature when sprayed coolant is introduced into the boundary layer (fog). $V_{wheel} = 50 \text{ m/s}$; b) circle temperature when sprayed coolant (fog) is introduced into the boundary layer. $V_{wheel} = 80 \text{ m/s}$.

3. Conclusions

Contact heat transfer between the circle and the boundary layer is not effective enough to reduce the temperature of the wheel

When air with negative temperature is introduced into the boundary layer by means of a Ranque-Hillsch tube, the wheel temperature decreases by about 10%.

A slight decrease in temperature during contact heat transfer between the cutting disc and the boundary layer is explained by a low coefficient of thermal conductivity of air. When a sprayed coolant is introduced into the boundary layer using an ejector tube (fog cooling), the wheel temperature decreases by 25%, which ensures an increase in the time of continuous operation.

4. Results

As a result of the study, it was found that to increase the time of continuous operation of the wheel, cooling of the boundary layer must shall be carried out using an ejector tube.

References

- [1] Shintaro Imayama R J, Lingwood P and Alfredsson H 2014 The turbulent rotating-wheel boundary layer *Europ J of Mech B/Fluids* **48** pp 245-53
- [2] Appelquist E, Schlatter P, Alfredsson P and Lingwood R 2018 Turbulence in the rotating-wheel boundary layer investigated through direct numerical simulations *Europ. J of Mech B/Fluids* **70** pp 6-18
- [3] Cebeci T and Abbott D 1975 Boundary layers on a rotating wheel *AIAA J* **1(6)** pp 561-67
- [4] Shintaro Imayama R J 2012 Experimental study of the rotating-wheel boundary-layer flow *Techn. Reports from Royal Inst. of Techn KTH Mech SE-100 44 60*
- [5] Parthasarathy R N 2002 Analysis of the turbulent boundary layer on a rotating wheel *Microsystem Techn* **8(4-5)** pp 278-81
- [6] Kohama Y 1984 Studies of the rotating-wheel boundary-layer flow *Acta Mech* **50** pp 193-99
- [7] Imayama S 2014 Studies of the rotating-wheel boundary-layer flow *Techn. Reports from Royal Inst of Techn KTH Mech SE-100 44 Stockholm 58*
- [8] Shevchuk I V 2009 Convective heat and mass transfer in rotating wheel systems *Springer Verlag* 239
- [9] Mehmood A and Usman M 2018 Heat transfer enhancement in rotating wheel boundary layer *Thermal Sci Year* **22(6)** pp 2467-82
- [10] Ong C L and Owen J M 1991 Computation of the flow and heat transfer due to a rotating disc *Int.l J. of Heat and Fluid Flow* **12(2)** pp 106-15
- [11] Harmand S, Pellé J, Poncet S and Shevchuk I 2013 Review of fluid flow and convective heat transfer within rotating wheel cavities with impinging jet *Int. J. of Thermal Sci.* **67** pp 1-30
- [12] Turkyilmazoglu M 2018 Fluid flow and heat transfer over a rotating and vertically moving wheel *Phys. of Fluids* **30** pp 603-5

- [13] Lebedev V, Bespalova A and Dashkoskaya O 2016 Regularities of dust formation during stone cutting for construction works *Odes'kyi Politech. Univer. Pratsi* **2(49)** pp 24-30
- [14] Bespalova A, Lebedev V, Tonkonogyi V, Morozov Y and Frolenkova O 2019 Cutting stone building materials and ceramic tiles with diamond disc *Proceedings of the 2nd Int. Conf. in Design, Simul., Manufacturing: The Innov. Exch. DSMIE-2019* pp 510-21
- [15] Bespalova A, Lebedev V, Frolenkova O and Chumachenko T 2019 Cutting stone and ceramic building materials with diamond discs. *Sci. letters of acad. society of M Baludansky* **7** pp 9-17
- [16] Bespalova A, Lebedev V, Morozov Y, Chumachenko T and Klymenko N 2019 Mathematical modeling of the process of the interaction of the cutting diamond wheel with the environment *Grabchenko's Intern. Conf. on Advance Manuf. Process, InterPartner-2019* pp 3-14